Science
AAAS

Supplementary Materials for

Assessing ExxonMobil's global warming projections

G. Supran, S. Rahmstorf, N. Oreskes

Correspondence to: gjsupran@fas.harvard.edu

This PDF file includes:

(S1) Methods and (S2) Materials
References (*87-119*)
Fig. S1
Tables S1 to S4

Other Supplementary Materials for this manuscript include the following:

(S4) Online Repository

(S1) Methods

S1.1 Content analysis and digitization

Having compiled document corpora as detailed in section S2.1, we conducted a manual content analysis of all documents using *NVivo* digital annotation software (*1*).

To do so, the coder read each document, including its text, figures, and tables. Coding was deductive, based on a coding scheme defined by our research questions, which were to evaluate the performance of global warming projections reported by ExxonMobil scientists in terms of (a) graphical overlays, (b) temperature versus time (and associated skill scores), (c) iTCR (and associated skill scores), and (d) when human-caused global warming would first be detectable. Accordingly, the codes were as follows:

1. Document publication year
2. Projected future radiative forcings (including at least atmospheric carbon dioxide (CO_2) concentration) versus time (including at least two points in time)
3. Projected future global mean surface temperature (GMST) versus time (including at least two points in time)
4. Projected future GMST versus future radiative forcings (including at least atmospheric CO_2 concentration)
5. Projected date when anthropogenic global warming would first be detectable
6. Attributed origin of reported climate model projections
   - 6.1. Internal (model built or run in-house by – or in collaboration with – ExxonMobil scientists)
   - 6.2. External (model built and run by third parties, such as independent academic/government scientists)

The quantitative nature of all coded projections (with the exception of code 6, which is binary and straightforward to assign based on whether any external sources were attributed) meant that their identification was not subjective. It was therefore deemed unnecessary to verify intercoder reliability.

The units of analysis and observation in our study were individual reported projections consistent with code 1 and one or more of codes 2-6. For models driven by more than one forcing time series (i.e. for high and low CO_2 scenarios as well as a central, 'nominal' one), each resulting GMST time series was treated as a separate and individual projection. Figs. 3 and S1 and Table 1 therefore distinguish between 'nominal', 'high', and 'low' model projections. By contrast, for a given CO_2 scenario, GMST time series accompanied by uncertainty bars (corresponding, for example, to different model climate sensitivities) were treated as single projections with uncertainty bounds given by those uncertainty bars. Sections S1.2.2 and 1.2.3 describe how these uncertainties were factored into our calculations of uncertainty bars in figs. 3 and S1.

The resulting 16 distinct GMST projections that we identified, presented by way of 12 unique graphs and one table, are summarized in section S2.2. Fig. 1 reproduces the 12 graphs, each overlayed with observed temperature changes.

Once identified, all original GMST and forcing projections were converted for analysis: graphs were digitized using the free online application WebPlotDigitizer (v.4.4), and tables were extracted to spreadsheets (*2*). All resulting raw data are provided in our online depository.

S1.2 Evaluation of model performance

In the following subsections, we outline our various approaches to evaluating the performance of global warming model projections reported by ExxonMobil scientists: (subsection S1.2.1) graphical overlays; (subsection S1.2.2) temperature-versus-time metric; (subsection S1.2.3) iTCR metric; (subsection S1.2.4) skill scores; (subsection S1.2.5) sensitivity analyses; and (subsection S1.2.6) detectable anthropogenic global warming forecasts. We adopt the methods of Hausfather *et al.* (2020) for computing and interpreting the temperature-versus-time metrics, the iTCR metrics, and skill scores, and direct the reader there for additional details (*3*) (the Intergovernmental Panel on Climate Change (IPCC) has since adopted similar methods (*4*)). In the relevant subsections below, as well as in section S2.2, we summarize these methods and describe ways in which they were tailored to accommodate the data at hand. Finally, in subsection S1.2.7, we discuss the implications and limitations of model-versus-observation comparisons.

Throughout our analysis, model projection periods were defined as starting on the publication year of the document containing each projection, and ending in 2019 (or in the final projected year, if earlier).

S1.2.1 Graphical overlays

As an initial, visual evaluation of the performance of global warming model projections reported by ExxonMobil scientists, we overlayed all original GMST time series with observed temperature changes (Figs. 1 and 2).

In Fig. 1, observations were aligned with respect to the earliest reference year(s) for which model projection data were available. The reference year(s) we used for each projection are provided in section S2.2. In panels 1a,2-12 of Fig. 1, the plotted observations reflect the smoothed (LOWESS: *span* = 0.3; time series length = 1850 to 2020; effective smoothing = $0.5 \times 0.3 \times (2020 - 1850) = 25.5$ years) annual average of five historical time series: Hadley/UEA HadCRUT4 (*5*); National Oceanic and Atmospheric Administration (NOAA) GlobalTemp (*6*); National Aeronautics and Space Administration (NASA) GISTEMP (*7*); Berkeley Earth (*8*); and Cowtan and Way (2014) (*9*). The observations in panel 1b of Fig. 1 reflect a smoothed (LOWESS: *span* = 0.001; time series length = –149,900 years to +25,000 years; effective smoothing = $0.5 \times 0.001 \times (149{,}900 + 25{,}000) = 87.5$ years) Earth system model simulation (Ganopolski and Brovkin (2017)) of the last 150,000 years driven by orbital forcing only, with an appended moderate anthropogenic emissions scenario (*10*).

Additionally, in panel 3 of Fig. 1, we overlay an Exxon-modeled projection of future atmospheric CO_2 concentration with historical annual mean observations from Mauna Loa Observatory (Scripps Institution of Oceanography and NOAA Earth System Research Laboratories) (*11*).

In Fig. 2, projections, shown in grey, are plotted from the observed temperature change, shown in red, at the start of each projection period. The plotted observations reflect the same smoothed annual average of five historical time series as in Fig. 1, zeroed at the first plotted year (1900).

S1.2.2. Temperature-versus-time

Each projected and observed GMST time series, $GMST_i(t)$, was fitted over the corresponding projection period with: (a) an ordinary least squares (OLS) model of the form $GMST_i = \beta_i t + \varepsilon_i$; and (b) a first-order autoregressive (AR1) model of the form $GMST_{i,t} = c + \rho GMST_{i,t-1} + \varepsilon_t$.

The OLS fit to each model projection yielded a trend (i.e. gradient) coefficient β. Multiplying this by 10 gave the projected per-decade temperature changes shown in Fig. 3A. The mean of all of these projections is displayed in the yellow-labeled box in Fig. 3A, along with uncertainty bars representing the bootstrapped two-sigma standard error of the mean. (For comparison, an equivalent mean and two-sigma standard error of the mean of mainstream model projections reported by Hausfather *et al.* (2020) is also shown in the yellow-labeled box in Fig. 3A (*3*).) OLS fits to the five above observational temperature records yielded the five equivalent coefficients $\beta_1 ... \beta_5$. Multiplying their mean, $\overline{\beta}$, by 10 gave the observed per-decade temperature changes shown in Fig. 3A.

For each model scenario available (nominal/high/low CO_2 emissions), uncertainty bars in Fig. 3A were (conservatively) equated to the larger of the AR(1) and OLS two-sigma trend uncertainties ($\pm 2 \cdot \sigma(GMST_{model})$), multiplied by 10. These upper (lower) trend uncertainties were computed as the differences between upper (lower) 95% confidence limits of regression coefficients and the coefficient best-estimates. For model scenarios accompanied by uncertainty bars (corresponding, for example, to different model climate sensitivities), the upper and lower trend uncertainties shown in Fig. 3A correspond to (a) the *upper* trend uncertainty of the *high end* of those uncertainty bars and (b) the *lower* trend uncertainty of the *low end* of those uncertainty bars, respectively.

For observed temperature changes over time, uncertainty bars in Fig. 3A were estimated by adding in quadrature (a) the two-sigma coefficient uncertainty and (b) the square of the mean of the AR(1) or OLS two-sigma trend uncertainties (whichever larger, as above, for each of the five observational temperature records), *viz.*:

$$\overline{\beta} \pm \sqrt{4 \cdot var(obs) + 4 \cdot \langle \sigma(GMST_i) \rangle^2} \quad (1)$$

where $var(obs)$ is the variance of $\beta_1 ... \beta_5$ and $2 \cdot \sigma(GMST_i)$ are the two-sigma trend uncertainties.

To determine whether projections are consistent with observations in terms of the temperature-versus-time metric, we calculate the differences between each projected temperature series and the five observed temperature records, yielding five temperature difference series. Trends and uncertainties for these difference series are then calculated just as they were above for the five observational series, yielding Fig. S1A (for model scenarios accompanied by uncertainty bars, difference series based on the high and low ends of these uncertainty bars were respectively used to calculate the upper and lower trend uncertainties in Fig. S1A). Projections and observations are deemed consistent only if the 95% confidence intervals of the differences include zero.

S1.2.3 Implied TCR

Implied transient climate response (iTCR) refers to the change in temperature versus change in radiative forcing. For each projected and observed GMST time series, it is calculated by regressing temperature against anthropogenic radiative forcing over the model projection period, and multiplying the result by the forcing associated with doubled atmospheric CO_2 concentrations, $F_{2x} = 3.7\ \mathrm{W/m^2}$ (*3*), *viz.*:

$$iTCR = F_{2x} \cdot \Delta T / \Delta F_{anthro} \quad (2)$$

For model projections, ΔF_{anthro} was based on explicit external forcing values when provided, and was otherwise estimated from model CO_2 concentration scenarios as:

$$\Delta F_{anthro} = 5.35 \cdot \ln\left(\frac{p'_{CO_2}}{p_{CO_2}}\right) \quad (3)$$

where p_{CO_2} is the initial CO_2 concentration (in parts per million) at the start of the projection period and p'_{CO_2} is the CO_2 concentration during each subsequent year through 2019 (*3*). Analogous to the temperature-versus-time metric, iTCR was calculated by OLS regression of projected temperature against anthropogenic forcing. Likewise, for each model scenario available (nominal/high/low CO_2 emissions), uncertainty bars in Fig. 3B were equated to OLS two-sigma trend uncertainties ($\pm 2 \cdot \sigma(TCR_{model})$) multiplied by $F_{2x} = 3.7\ \mathrm{W/m^2}$ (an autoregressive model is not used here because it requires a time variable). As before, these upper (lower) trend uncertainties were computed as the differences between upper (lower) 95% confidence limits of regression coefficients and the coefficient best-estimates. Also as before, for model scenarios accompanied by uncertainty bars, the upper and lower trend uncertainties shown in Fig. 3B correspond to (a) the *upper* trend uncertainty of the *high end* of those uncertainty bars and (b) the *lower* trend uncertainty of the *low end* of those uncertainty bars, respectively.

Following Hausfather *et al.* (2020), ΔF_{anthro} included only anthropogenic forcings and excluded volcanic and solar changes, which avoided introducing sharp interannual changes in forcing that would complicate interpretation of iTCR over short time periods (*12*). Observed ΔF_{anthro} were based on a 1,000-member ensemble of observationally informed forcing estimates reported by Dessler and Forster (2018) through 2017 and extracted by Hausfather *et al.* (2020) (*12*). We extrapolated this ensemble through 2019 using an Autoregressive Integrated Moving Average (ARIMA) time series forecasting model. These 1000 ensemble members were then each regressed against each of the five observational temperature records using an OLS model, yielding 5,000 estimates of $\Delta T / \Delta F_{anthro}$, $\beta_1 ... \beta_{5000}$. Multiplying their mean, $\overline{TCR_{obs}}$, by $F_{2x} = 3.7\ \mathrm{W/m^2}$ gave the observed iTCR values shown in Fig. 3B. Uncertainty bars in Fig. 3B were estimated by adding in quadrature (a) the two-sigma coefficient uncertainty and (b) the square of the mean of the OLS two-sigma trend uncertainties of the 5,000 regression coefficients, *viz.*:

$$\overline{iTCR_{obs}} \pm \sqrt{4 \cdot var(iTCR_{obs})} \quad (4)$$

$$\sqrt{var(iTCR_{obs})} = \sqrt{var(obs) + \langle \sigma(GMST_i) \rangle^2} \quad (5)$$

where $var(obs)$ is the variance of $\beta_1 ... \beta_{5000}$ and $2 \cdot \sigma(TCR_i)$ are the two-sigma OLS trend uncertainties.

To determine whether projections are consistent with observations in terms of the iTCR metric, we calculate:

$$iTCR_{diff} \pm \sqrt{4 \cdot var(iTCR_{model}) + 4 \cdot var(iTCR_{obs})} \quad (6)$$

where $var(iTCR_{model})$ and $var(iTCR_{obs})$ are as defined above and

$$iTCR_{diff} = iTCR_{model} - \overline{iTCR_{obs}} \quad (7)$$

This yielded Fig. S1B. Projections and observations are again deemed consistent only if the 95% confidence intervals of the differences include zero. As before, for model scenarios accompanied by uncertainty bars, difference series based on the high and low ends of these uncertainty bars were respectively used to calculate the upper and lower trend uncertainties in Fig. S1B).

S1.2.4 Skill scores

We calculate the 'skill score' (*SS*) of each model as defined by Hargreaves (2010) (*13*). The skill score compares the root-mean-squared errors of a model projection, E_f, with those of a zero temperature change null hypothesis, E_{ref}, and is defined as:

$$SS = 1 - \sqrt{E_f / E_{ref}} \quad (8)$$

where

$$E_f = (\beta_{obs} - \beta_{model})^2 \quad (9)$$

$$E_{ref} = (\beta_{obs} - 0)^2 \quad (10)$$

and β_{obs} and β_{model} are the OLS trend coefficients of given observation and model projection datasets, respectively.

For each projection, we calculate skill scores with respect to: (a) each of the five observational temperature records, for the temperature-versus-time metric; and (b) with respect to the 5,000 estimates of $\Delta T / \Delta F_{anthro}$, for the iTCR metric. For each projection and metric, the median of these skill scores is presented in Table 1. The mean average of these skill scores is computed across: (a) all 16 projections reported by ExxonMobil scientists; (b) all 16 projections bar two overlaps with the 18 academic/government projections analyzed by Hausfather *et al.* (2020) (see section S1.2.5 and Table S1 for details); and (c) the 12 projections modeled by ExxonMobil scientists themselves (indicated by asterisks in Table 1). Mean average skill scores are reported together with bootstrapped one-sigma standard errors of the means.

Uncertainties in skill scores are estimated using a Monte Carlo approach. For the temperature-versus-time metric (iTCR metric), for each of the five observational temperature records (5,000 estimates of $\Delta T / \Delta F_{anthro}$) we generate 100 random samples of the Gaussian distribution of the

corresponding OLS regression coefficient and compute each corresponding skill score. The 5th and 95th percentiles of these skill scores serve as the confidence intervals shown in Table 1. For clarity of presentation, all skill scores are reported as percentages.

S1.2.5 Sensitivity analyses

As noted above, two (out of 16) projections reported by ExxonMobil scientists overlap with the 18 academic and government climate model projections analyzed by Hausfather *et al.* (2020): "1982 Weinberg; 1984 Callegari | nominal" (which was reproduced from Hansen *et al.* (1981)) and "2001 Albritton | nominal" (*14*). To test the robustness of our findings, we excluded these two overlaps from our dataset and recalculated all reported statistics: (1) average predicted global warming; (2) uncertainty of global warming projections (bootstrapped two-sigma standard error of the mean); (3) fraction of projections consistent with historical observations; and (4) average skill score. (3) and (4) are computed for both temperature-versus-time and implied transient climate response (iTCR) metrics. As another sensitivity analysis of the accuracy and modeling skill of ExxonMobil's global warming projections, we also recalculated all of the above statistics for only the 12 (out of 16) temperature projections specifically output by models built or run in-house by ExxonMobil scientists, indicated by asterisks in Figs. 1–3 and Table 1 and discussed in the main text. All sensitivity analysis results are reported in Table S1.

S1.2.6 Detectable warming analysis

Table S4 summarizes the ten internal reports and one peer-reviewed publication found to offer numerical estimates as to when human-caused global would first be detectable. For each document, the predicted year is inferred from its corresponding supporting quotations. The median predicted year is reported together with the bootstrapped two-sigma standard error of the median.

S1.2.7 Implications and limitations of model-versus-observation comparisons

Retrospectively comparing model projections to observations offers a robust, independent, and established test of model skill. This is because a primary factor influencing both temperature-versus-time and iTCR metrics is the accuracy of each model's physics, including sensitivity of the climate to external forcings and the resolution or parameterization of physical processes such as heat uptake by the deep ocean (*3*). It is important to note, however, that model-versus-observation differences can also arise due to other factors (*15–17*). In particular, the performance of model temperature projections also depends on the accuracy of projected changes in anthropogenic external forcing due to greenhouse gases and aerosols, and on the natural forcing arising from solar irradiance changes and volcanic aerosols (*3*, *18*, *19*). The iTCR metric accounts for potential mismatches in projected anthropogenic emissions, but potential errors in observed forcing estimates – because ΔF_{anthro} do not include natural forcings – add uncertainty to the iTCR comparison, particularly on shorter timescales (*18*). Nonetheless, following Hausfather *et al.* (2020), we observe that with two exceptions (Kheshgi and Jain (2003), figs. 7c and 8c), all of the nominal CO_2 scenario projections reported by ExxonMobil have rates of external forcing increase in the projection period between 1–1.4 times of the mean estimate of observational forcings, and thus likely exist in the regime where iTCR depends largely on radiative feedbacks and ocean heat uptake (*3*). Moreover, several studies suggest that the temperature response to twentieth century anthropogenic forcing falls within this regime (*3*, *20*). Indeed, the key reason that projections of anthropogenic warming are capable of closely matching observed warming is that natural climate changes are estimated to have played a minor

role over the full time period concerned here: since the late nineteenth century, global warming has been almost entirely human-caused (*21*, *22*). Fortuitously, the magnitude of total anthropogenic forcing is, within current estimates of the uncertainty in that forcing, similar to the magnitude of CO_2 forcing alone, because the warming effects of other greenhouse gases and the cooling effects of other sources (mostly aerosols) roughly cancel one another out (*23*). This is why even CO_2-only simulations can match observed warming quite well.

Finally, we note that model-versus-observation differences in both temperature trends and iTCR are also affected by the quality of GMST observations, by incomplete observational coverage in space and varying coverage over time, and by the fortuitous phasing of internal variability in the real world (*24*, *25*).

(S2) Materials

2.1 Corpora

For a detailed description of how we previously compiled the 104 ExxonMobil documents analyzed in this study, see refs. (*26*, *27*). In summary, the 32 internal company documents (1977–2002) were collated from public archives provided by ExxonMobil Corp (*28*), *InsideClimate News* (*29*), and Climate Investigations Center (*30*). The 72 peer-reviewed publications (1982–2014) were obtained by identifying all peer-reviewed documents among ExxonMobil Corp's lists of 'Contributed Publications', except for three articles discovered independently during our research (all 72 publications were (co-)authored by at least one ExxonMobil employee) (*31*).

Raw data (original PDF internal documents and peer-reviewed publications) for this study cannot be reproduced due to copyright restrictions. However, Tables S2-3 present catalogs of all 104 analyzed documents, which can be obtained at the following public archives:

- All analyzed internal documents can be downloaded from (one or more of) ExxonMobil Corp (*28*), *InsideClimate News* (*29*), and Climate Investigations Center (*30*).
- All analyzed peer-reviewed documents can be obtained from corresponding journals and conference proceedings.

2.2 Individual projection details

In this section, we provide detailed information about all global warming projections reported by ExxonMobil scientists identified by our content analysis and evaluated in this study. For each projection, the following are variously documented as relevant: (i) temperature data (sources, scenarios and/or uncertainty bars, summary of data preparation); (ii) CO_2 data (sources and summary of data preparation); (iii) origin of projected data (internal or external, cf. code 6 in section S1.1); (iv) type of temperature response (transient or equilibrium); (v) projection period; (vi) reference period for graphical overlay in Fig. 1; and (vii) additional notes regarding methodological details.

Black (1977, vugraph 10); Mastracchio (1979) (as in Fig. 1, panel 1a)

- *Temperature data*
  - Sources
    - Black (1977) (*32*): vugraph 10

    - Mastracchio (1979) (*33*): fig. 4
  - Scenarios and/or uncertainty bars
    - Nominal scenario: "Estimated global mean temperature" ("Estimated polar regions temperature" is not included).
    - Nominal scenario uncertainty bars: upper and lower uncertainty bars of the "Estimated global mean temperature" curve.
  - Summary: We digitize and linearly interpolate this temperature data (equivalent in the two documents) to generate annual values.
- *CO_2 data*
  - Sources
    - Black (1977) (*32*)
      - Page 1: "The earth's atmosphere presently [1977] contains about 330 ppm of CO_2."
      - Page 2: "It can be estimated that since 1850 the concentration of this gas [CO_2] in the atmosphere has increased by about 13%." This implies a CO_2 concentration of $330/1.14 \approx 292$ ppm in 1850.
      - Page 6: "The extrapolations past 1977 result from the application of Wanabe and Wetherald's model with the assumption that the carbon dioxide levels will double by 2050 A.D." This implies a CO_2 concentration of $\sim 292 \times 2 = 584$ ppm in 2050.
    - Mastracchio (1979) (*33*)
      - Fig. 7: "Rate of CO_2 buildup" for an "unlimited increase" scenario.
      - Page 5: "…the preindustrial concentration of [CO_2 was] 290 ppm."
      - Page 3: "Many models today predict that doubling the 1860 atmospheric CO_2 concentration will cause a 1° to 5°C global temperature increase (see Figure 4). Extrapolation of present fossil fuel trends would predict this doubling of the CO_2 concentration to occur about 2050." This implies a CO_2 concentration of $290 \times 2 = 580$ ppm in 2050.
    - Summary: Since Mastracchio (1979) explicitly links the temperature data in fig. 4 to the "No limit on CO2 emissions" scenario described on page 5 and depicted in fig. 7 (wherein a "doubling of the pre-industrial concentration [of CO_2 to ~580 ppm] occurs around 2050"), and since this is essentially consistent with Black (1977)'s assumption of 584 ppm in 2050, our analysis uses the more detailed CO_2 data in fig. 7 of Mastracchio (1979). We digitize and linearly interpolate that data to generate annual values.
- *Origin of projection data*: External. Figure is reproduced from fig. 7 of Kellogg (1977) (which Black (1977) cites as ref. 12) (*34*). The caption to fig. 7 of Kellogg (1977) says that it is adapted from Mitchell Jr. (1977) (which Black (1977) cites as ref. 13) (*35*).
- *Temperature response*: Transient (graph plots "change of surface temperature from present").
- *Projection period*: 1977–2019
- *Reference years for graphical overlay*: 1850–1900
- *Notes*: The July 1977 presentation by Exxon scientist James Black to the Exxon Corporation Management Committee is documented and described by Black in a June 1978 memo (*32*). Thus, the start of the projection period is 1977, but the formal publication date of the memo is 1978. To avoid confusion, we refer to this document here and throughout as Black (1977).

Black (1977, vugraph 11) (as in Fig. 1, panel 1b)

- *Temperature data*
  - Source: Black (1977) (*32*), vugraph 11
  - Summary: This dataset was not included in our quantitative analysis because its 150,000-year timescale does not permit accurate digitization of its projected post-Industrial anthropogenic global warming.
- *Origin of projection data*: External. Figure is reproduced from Mitchell Jr. (1977) (which Black (1977) cites as ref. 13) (*35*).
- *Temperature response*: Equilibrium, effectively – this is a graph of the global warming "effect of CO_2 on an interglacial scale."
- *Reference years for graphical overlay*: pre-Industrial Revolution

Shaw (1980); Glaser (1982, fig. 9) (as in Fig. 1, panel 2)

- *Temperature data*:
  - Sources
    - Shaw (1980) (*36*): fig. 7
    - Glaser (1982) (*37*): fig. 9
  - Scenarios and/or uncertainty bars
    - Nominal scenario: The centerline of the "Expected range of fluctuations including CO_2 effect", calculated as a line beginning at the end of the "Observed past changes" curve and thereafter vertically bisecting the "expected range".
    - Nominal scenario uncertainty bars: upper and lower bounds of the "expected range".
  - Summary: We digitize and linearly interpolate this temperature data (equivalent in the two documents) to generate annual values.
- *CO_2 data*:
  - Sources
    - Shaw (1980) (*36*)
      - Page 1: "There is, however, great uncertainty on whether the atmospheric CO_2 concentration prior to the Industrial Revolution was 290-300 ppm or 260-270 ppm."
      - Fig. 1 and page 1: "In addition to observing a trend between 1957-1979 that showed atmospheric CO_2 increasing from 315 to 337 ppm…". The 1979 CO_2 concentration is therefore taken to have been 337 ppm.
      - Page 2: "Calculations recently completed at Exxon Research indicate that using the energy projections from the CONAES study and the World Energy Conference, a doubling of atmospheric CO2 can occur at about 2060. If synthetic fuels are not developed, and fossil fuel needs are met by petroleum, then the atmospheric CO2 doubling time would be delayed by about 5 years to 2065." Assuming a pre-Industrial CO_2 concentration of ~290 ppm, this implies a concentration of $\sim 290 \times 2 = 580$ ppm in 2050.
    - Glaser (1982) (*37*)
      - Page 2: "…to observing a trend between 1957-1979 that showed atmospheric CO_2 increasing from 315 to 337 ppm…". The 1979 CO_2 concentration is therefore taken to have been 337 ppm.
      - Page 1: "We estimate doubling [of CO_2] could occur around the year 2090 based upon fossil fuel requirements projected in Exxon's long range energy outlook." This implies a concentration of $\sim 337 \times 2 = 674$ ppm in 2090.

    - Summary: Although Glaser (1982) presents updated CO_2 projections compared to Shaw (1980), it is not clear that they were available at the start of the projection period. Our analysis therefore uses the CO_2 values from Shaw (1980): 337 ppm in 1979; and 580 ppm in 2050. We first use eq. 3 to convert this change in CO_2 concentrations into a radiative forcing. Then, assuming a linear relationship between temperature and forcing (as inherent to calculating iTCR), we use the corresponding temperature projections to linearly interpolate changes in radiative forcing throughout the projection period.
- *Origin of projection data*: External. Figure is reproduced from Mitchell Jr. (1977), although no citation is provided in either document (*35*).
- *Temperature response*: Transient (figure caption in both documents is "projected instantaneous climatic response to increasing CO_2 concentrations").
- *Projection period*: 1980–2019
- *Reference years for graphical overlay*: 1850–1900
- *Notes*: For this dataset only, the AR(1) model fit does not compute due to, by coincidence, perfectly correlated data. We therefore take a conservative approach to estimating uncertainties by computing trend uncertainty based on OLS rather than AR(1) confidence intervals, which are ~O(10^{-16} °C/decade) versus ~O(0.02 °C/decade), respectively. This leads to only a minor narrowing (<10%) of the overall uncertainty bars displayed in Fig. 3, owing to the much larger coefficient uncertainties (~0.34 °C/decade) arising from the difference in slopes of the upper and lower bounds of the scenarios.

Glaser (1982, fig. 3/table 4); Shaw (1984) (as in Fig. 1, panel 3)

- *Temperature data*
    - Sources
        - Glaser (1982) (*37*): fig. 3/table 4
        - Shaw (1984) (*38*): graph on page 9
    - Scenarios and/or uncertainty bars
        - Nominal scenario: "Most probable temperature increase" (21st Century Study case), both for temperature and CO_2.
    - Summary: We digitize and linearly interpolate this temperature data (equivalent in the two documents) to generate annual values.
- *CO_2 data*
    - Sources
        - Glaser (1982) (*37*): fig. 3/table 4
        - Shaw (1984) (*38*): graph on page 9
    - Summary: We digitize and linearly interpolate this CO_2 data (equivalent in the two documents) to generate annual values.
- *Origin of projection data*: Internal. No third-party source is cited. Shaw (1984) presents the graph in the context of "results" of "Exxon" work compared against "EPA", "NRC/NAS", and "MIT". Figures in both Glaser (1982) and Shaw (1984), and the text of Glaser (1982), attribute the temperature projection data to Exxon's "21st Century Study" "based on the Exxon 21st Century Study-High Growth scenario". The text of Glaser (1982) attributes the CO_2 data in the figure to "Calculations recently completed at Exxon Research and Engineering Company using the energy projections from the Corporate Planning Department's 21st Century Study". Shaw (1984) describes the CO_2 and temperature

projections "as part of CPPD's [*sic*: Corporate Planning Department] technology forecasting activities in 1981".

- *Temperature response*: Transient (in Shaw (1984), the graph is entitled "instantaneous global temperature increase as a function of time").
- *Projection period*: 1982–2019
- *Reference years for graphical overlay*: 1979
- *Notes*: Graphically overlaying data from fig. 3 and table 4 in Glaser (1982) showed that their projections are equivalent. These datasets were therefore treated as a single projection.

Weinberg et al. (1982); Callegari (1984) (as in Fig. 1, panel 4)

- *Temperature data*
  - Sources
    - Weinberg *et al.* (1982) (*39*): graph on page 7
    - Callegari (1984) (*40*): graph on page 8
  - Scenarios and/or uncertainty bars
    - Nominal scenario: Solid centerline ($\Delta T = 2.8$°C model sensitivity in Hansen *et al.* (1981) (*14*))
    - Nominal scenario uncertainty bars: Upper bound given by upper (dashed) line ($\Delta T = 5.6$°C model sensitivity in Hansen *et al.*); lower bound given by lower (dotted-dashed) line ($\Delta T = 1.4$°C model sensitivity in Hansen *et al.*).
  - Summary: We digitize and linearly interpolate this temperature data (equivalent in the two documents) to generate annual values.
- *CO_2 data*
  - Since the temperature projections were originally reported by Hansen *et al.* based on their "slow-growth" (2a) scenario, we use CO_2 concentrations for this scenario calculated by Hausfather *et al.* (2020) based on the conversion factors in table 2 of Hansen *et al*. (*3*)
- *Origin of projection data*: External. Figure is reproduced from Hansen *et al.* (1981) (cited in Callegari (1984) (*40*)).
- *Temperature response*: Transient
- *Projection period*: 1982–2019
- *Reference years for graphical overlay*: 1950–1970

Flannery (1985, page 23) (*41*) ***(as in Fig. 1, panel 5)***

- *Temperature data*
  - Source: Graph on page 23: "temperature change with UD [upwelling diffusion] model"
  - Scenarios and/or uncertainty bars
    - Nominal scenario: "Actual" temperature change curve for "Nominal CO_2"
  - Summary: We digitize and linearly interpolate this temperature data to generate annual values.
- *CO_2 data*
  - Source: Graph on page 22: "CO2 record and forecasts from Wuebbles (SOA Report)"
  - Summary: We digitize and linearly interpolate this CO_2 data to generate annual values.
- *Origin of projection data*: Internal. Figure is based on Exxon's own collaborative modeling work with Martin Hoffert (New York University). The graph is presented as part of "CR Research 1984-85" and reflects Exxon's "collaborative development of a sophisticated Energy Balance Climate Model" with "Livermore, NYU" [Lawrence Livermore National

Laboratory and New York University]. The upwelling-diffusion model used here was initially developed by Hoffert, Callegari, and Hsieh (1980) (*42*). That same year, Callegari joined Exxon (*43*).

- *Temperature response*: Transient (figure shows "actual" "temperature change with UD [upwelling-diffusion] model", and compares this to "equilibrium" temperature change").
- *Projection period*: 1985–2019
- *Reference years for graphical overlay*: 1850
- *Notes*:
  - Graphically overlaying data from pages 23 and 24 of Flannery (1985) showed that their projections are distinct. These datasets were therefore treated as separate projections.
  - The time axis appears to have been mislabeled (years ending in '60s should, it seems, have been '50s) because the labels disagree with those in the peer-reviewed publication resulting from this collaboration, Hoffert and Flannery (1985), and because otherwise the implied time intervals are non-uniform (*44*). We therefore assumed that axis ticks indicating '60s actually correspond to '50s when digitizing the plot.
  - The temperature projection on page 22 of Flannery (1985) is "change in equilibrium [versus transient] temperature," and was therefore not included in our analysis.

Flannery (1985, page 24) (*41*) ***(as in Fig. 1, panel 6)***

- *Temperature data*
  - Source: Graph on page 24: "Temperature change for various CO2 forecasts"
  - Scenarios and/or uncertainty bars
    - Nominal scenario: "Nominal" temperature change curve
    - High scenario: "High" temperature change curve
    - Low scenario: "Low" temperature change curve
  - Summary: We digitize and linearly interpolate this temperature data to generate annual values.
- *CO_2 data*
  - Source: Graph on page 22: "CO2 record and forecasts from Wuebbles (SOA Report)"
  - Summary: We digitize and linearly interpolate this CO_2 data to generate annual values.
- *Origin of projection data*: Internal. Figure is based on Exxon's own collaborative modeling work with Martin Hoffert (New York University). The graph is presented as part of "CR Research 1984-85". The upwelling-diffusion model used here was initially developed by Hoffert, Callegari, and Hsieh (1980) (*42*). That same year, Callegari joined Exxon (*43*).
- *Temperature response*: Transient (figure shows same "actual" "temperature change with UD [upwelling diffusion] model" as on page 23 of Flannery (1985), but "for various CO2 forecasts."
- *Projection period*: 1985–2019
- *Reference years for graphical overlay*: 1850
- *Notes*:
  - Graphically overlaying data from pages 23 and 24 of Flannery (1985) showed that their projections are distinct. These datasets were therefore treated as separate projections.
  - The time axis appears to have been mislabeled (years ending in '60s should, it seems, have been '50s) because the labels disagree with those in the peer-reviewed publication resulting from this collaboration, Hoffert and Flannery (1985), and because otherwise the implied time intervals are non-uniform (*44*). We therefore assumed that axis ticks indicating '60s actually correspond to '50s when digitizing the plot.

Hoffert and Flannery (1985, fig. 5.16A) (*44*) ***(as in Fig. 1, panel 7a)***

- *Temperature data*
  - Source: Fig. 5.16A
  - Scenarios and/or uncertainty bars
    - Nominal scenario: "Nominal CO_2" temperature change curve
    - High scenario: "High CO_2" temperature change curve
    - Low scenario: "Low CO_2" temperature change curve
  - Summary: We digitize and linearly interpolate this temperature data to generate annual values.
- *CO_2 data*
  - Source: Table 5.2
  - Summary: We calculate annual CO_2 values based on the equations in table 5.2, which, as described in the table's caption, represent the emissions scenarios of Wuebbles *et al.* (1984).
- *Origin of projection data*: Internal. Figure is based on Exxon's own collaborative modeling work with Martin Hoffert (New York University), co-reported in this document with Hoffert. The upwelling-diffusion model used here was initially developed by Hoffert, Callegari, and Hsieh (1980) (*42*). That same year, Callegari joined Exxon (*43*).
- *Temperature response*: Transient (figure shows "transient temperature response to CO_2 forcing…computed with transient upwelling-diffusion (UD) ocean model of Hoffert *et al.* (1980)…").
- *Projection period*: 1985–2019
- *Reference years for graphical overlay*: 1859
- *Notes*:
  - Graphically overlaying data from figs. 5.16A and 5.16B of Hoffert and Flannery (1985) confirmed that the "Nominal CO_2" curve in fig. 5.16A and the "2.2 W m^{-2} K^{-1}" curve in fig. 5.16B are equivalent, whereas the other curves are distinct. The "Nominal CO_2" curve and the "2.2 W m^{-2} K^{-1}" curve were therefore treated as a single "nominal" projection, whereas the "High CO_2" and "Low CO_2" curves were treated as separate projections.
  - The time series displayed in Fig. 2 is "2.2 W m^{-2} K^{-1}", with upper bound = "4.4 W m^{-2} K^{-1}" and lower bound = "1.1 W m^{-2} K^{-1}". All three time series ("Nominal CO_2", "High CO_2", and "Low CO_2") are represented in Figs. 3 and S1 and in Table 1.
  - The temperature projection in fig. 5.6 of Hoffert and Flannery (1985) shows "global equilibrium [versus transient] temperature change versus time," and was therefore not included in our analysis.

Hoffert and Flannery (1985, fig. 5.16B) (*44*) ***(as in Fig. 1, panel 7b)***

- *Temperature data*
  - Source: Fig. 5.16B
  - Scenarios and/or uncertainty bars
    - Nominal scenario: "2.2 W m^{-2} K^{-1}" temperature change curve (equivalent to "Nominal CO_2" curve in fig. 5.16A – see notes for fig. 5.16A above)
    - Nominal scenario uncertainty bars: Upper bound given by "1.1 W m^{-2} K^{-1}" temperature change curve; lower bound given by "4.4 W m^{-2} K^{-1}" temperature change curve.

- Summary: We digitize and linearly interpolate this temperature data to generate annual values.
- *CO_2 data*
  - Source: Table 5.2
  - Summary: We calculate annual CO_2 values based on the equations in table 5.2, which, as described in the table's caption, represent the emissions scenarios of Wuebbles *et al.* (1984).
- *Origin of projection data*: Internal. Figure is based on Exxon's own collaborative modeling work with Martin Hoffert (New York University), co-reported in this document with Hoffert. The upwelling-diffusion model used here was initially developed by Hoffert, Callegari, and Hsieh (1980) (*42*). That same year, Callegari joined Exxon (*43*).
- *Temperature response*: Transient (figure shows "transient temperature response to CO_2 forcing…computed with transient upwelling-diffusion (UD) ocean model of Hoffert *et al.* (1980)…").
- *Projection period*: 1985–2019
- *Reference years for graphical overlay*: 1859

Jain et al. (1994) (*45*) ***(as in Fig. 1, panel 8)***

- *Temperature data*
  - Source: Fig. 7a
  - Scenarios and/or uncertainty bars
    - Nominal scenario: The centerline of the "4.5" and "1.5" °C model sensitivity responses to the Intergovernmental Panel on Climate Change (IPCC)'s "IS92a Scenario". The centerline was calculated so as to vertically bisect the "4.5" and "1.5" curves.
    - Nominal scenario uncertainty bars: Upper bound given by the "4.5" curve; lower bound given by the "1.5" curve.
  - Summary: We digitize and linearly interpolate this temperature data to generate annual values.
- *CO_2 data*
  - Source: Fig. 6b, IS92a scenario
  - Summary: We digitize and linearly interpolate this CO_2 data to generate annual values.
- *Origin of projection data*: Internal. Figure is based on Exxon's own collaborative modeling work with Atul Jain and Donald Wuebbles (Lawrence Livermore National Laboratory). The report presents an "Integrated Science Model which consists of coupled modules for carbon cycle, atmospheric chemistry of other trace gases, radiative forcing by greenhouse gases, energy balance model for global temperature, and a model for sea level response." The "globally averaged energy balance climate model" was "developed by Harvey and Schneider".
- *Temperature response*: Transient (the "Integrated Science Model presented in this report…is used to estimate the relation between the time-dependent rate of greenhouse gas emissions and quantitative features of climate – global temperature, the rate of temperature change…").
- *Projection period*: 1994–2019
- *Reference years for graphical overlay*: 1990

Kheshgi et al. (1997) (*46*) ***(table not shown in Fig. 1)***

- *Temperature data*
  - Source: Table 1
  - Scenarios and/or uncertainty bars
    - Nominal scenario: "Global temperature (C)" change in E_{A+1}+E_{N+4} scenario, comparable to the IPCC's IS92a business-as-usual scenario (see fig. 3 of Kheshgi *et al.* (1997)).
  - Summary: We linearly interpolate this temperature data to generate annual values.
- *CO_2 data*
  - Source: Table 1 (for change in CO_2 concentration); Keeling *et al.* (for initial, absolute CO_2 concentration in 1995)
  - Summary: We linearly interpolate this CO_2 data to generate annual values
- *Origin of projection data*: Internal. Figure is based on Exxon's own collaborative modeling work with Atul Jain and Donald Wuebbles (University of Illinois) using the Integrated Science Assessment Model (ISAM) developed through the same collaboration (*45*, *47*).
- *Temperature response*: Transient ("Table 1 shows the modeled change in global-mean temperature (realized temperature), global-mean equilibrium temperature…" – we use the former).
- *Projection period*: 1997–2010
- *Reference years for graphical overlay*: N/A (table does not permit graphical overlay)
- *Notes*:
  - To determine absolute CO_2 concentrations over time, we need the initial, absolute CO_2 concentration in 1995. To this end, we note that the authors of this paper (Kheshgi, Jain, and Wuebbles) co-authored another paper in our corpus, in 1996 (Jain, Kheshgi, and Wuebbles, *Tellus* 48B, 583-600), in which they plot (figure 2) "observed atmospheric CO_2" based on the citation of Keeling *et al.* (Nature 375, 666-670 (1995)). Keeling *et al.*'s paper presents CO_2 concentration through November 1994, making clear that Kheshgi *et al.* had access to Keeling *et al.*'s contemporary data. We therefore use Keeling *al.*'s 1995 average CO_2 concentration of 360.82 ppm [from https://perma.cc/K8VR-YU3U].

Albritton et al. (2001) (*48*) ***(as in Fig. 1, panel 10)***

- *Temperature data*
  - Source: Digitized version of fig. 22a of Technical Summary and, equivalently, fig. 5d of Summary for Policymakers, as reported by Hausfather *et al.* (2020) (*3*).
  - Scenarios and/or uncertainty bars
    - Nominal scenario: A2 SRES scenario. Like Hausfather *et al.*, we use this scenario because it has the most unique model runs available. We used the temperature time series reported by Hausfather *et al.*, which is an interpolated version of table II.4, Appendix II, Albritton *et al.* (2001).
    - Nominal scenario uncertainty bars: Upper and lower bounds are given by the "Model ensemble all SRES envelope" in the figure. We used the temperature time series reported by Hausfather *et al.*, which is a digitized version of this envelope.
  - Summary: We linearly interpolate this temperature data to generate annual values.
- *Radiative forcing data*
  - Source: A2 SRES scenario, Table II.3.11, Appendix II, Albritton *et al.* (2001).
  - Summary: We linearly interpolate this radiative forcing data to generate annual values.

- *Origin of projection data*: External. Figure is based on several independent models.
- *Temperature response*: Transient
- *Projection period*: 2001–2019
- *Reference years for graphical overlay*: 1990
- *Notes*: ExxonMobil Corp's chief climate scientist Haroon S. Kheshgi co-"prepared" the draft Summary for Policymakers of Albritton *et al.* (2001) and was a Contributing Author of its Technical Summary.

Kheshgi and Jain (2003, fig. 7c) (*49*) ***(as in Fig. 1, panel 11)***

- *Temperature data*
  - Source: Fig. 7c
  - Scenarios and/or uncertainty bars
    - Nominal scenario: Solid (central) line ("driven by the benchmark emission scenario IS92a)
    - Nominal scenario uncertainty bars: Upper bound is given by the upper dashed line, corresponding to the "highest projection" ("high parameterization of ISAM" model); lower bound is given by the lower dashed line, corresponding to the "lowest projection" ("low parameterization of ISAM" model).
  - Summary: We digitize and linearly interpolate this temperature data to generate annual values.
- *CO_2 data*
  - Fig. 7b (solid "Reference" curve)
  - Summary: We digitize and linearly interpolate this CO_2 data to generate annual values.
- *Origin of projection data*: Internal. Figure is based on ExxonMobil Corp's own collaborative modeling work with Atul Jain (University of Illinois). The paper presents a globally aggregated "Reduced Form Carbon/Climate System Model ISAM" (Integrated Science Assessment Model).
- *Temperature response*: Transient
- *Projection period*: 2003–2019
- *Reference years for graphical overlay*: 1856-75 (as defined in the paper)

Kheshgi and Jain (2003, fig. 8c) (*49*) ***(as in Fig. 1, panel 12)***

- *Temperature data*
  - Source: Fig. 8c
  - Scenarios and/or uncertainty bars
    - Nominal scenario: Orange line ("driven by the…IPCC SRES" A1B scenario). We use scenario A1B because it is only for this scenario that upper/lower bound projections are also reported. As Hausfather *et al.* (2020) have noted, over the 2003-19 projection period analyzed, the differences between A1B and A2 scenarios (the latter used in our analysis of Albritton *et al.* (2001) above) are minor.
    - Nominal scenario uncertainty bars: Upper and lower bounds are given by the grey envelope corresponding to "the highest and lowest projections (high and low parameterizations of ISAM)" for scenario A1B.
  - Summary: We digitize and linearly interpolate this temperature data to generate annual values.
- *CO_2 data*

  - Fig. 8b (A1B SRES scenario)
  - Summary: We digitize and linearly interpolate this CO_2 data to generate annual values.
- *Origin of projection data*: Internal. Figure is based on ExxonMobil Corp's own collaborative modeling work with Atul Jain (University of Illinois). The paper presents a globally aggregated "Reduced Form Carbon/Climate System Model ISAM" (Integrated Science Assessment Model).
- *Temperature response*: Transient
- *Projection period*: 2003–2019
- *Reference years for graphical overlay*: 1856-75 (as defined in the paper)

Miscellaneous numerical global warming projections not included in analysis

The following numerical global warming projections were not included among those evaluated in this study because they do not provide sufficient information to be consistent with codes 2-4 in section S1.1; most, for example, do not include temperatures and forcings for at least two points in time). Although they are not therefore amenable to our analyses, we list them here for completeness.

- Shaw (1981) (*50*)
  - Page 2: "Atmospheric CO_2 will double in 100 years if fossil fuels grow at 1.4%/a. 3°C global average temperature rise and 10°C at poles if CO_2 doubles."
- Shaw (1984, page 6) (*38*)
  - "Results/Effects" table on page 6: "Average temperature rise" due to "CO_2 doubling": 1.3–3.1°C in 2090.
- Flannery (1985, page 14) (*41*)
  - Page 14: "Consensus prediction": 1°C temperature rise by 1860–2000; 2–5°C temperature rise by 2100.
- Carlson (1988) (*51*)
  - Page 4: "Climate models predict a 1.5°C to 4.5°C global temperature increase in 100 years – depending on the projected growth in fossil fuel use"
- Kheshgi (1993) (*52*)
  - Eq. 1: "$\Delta T = S(t; \Delta Q) \cdot \Delta T_{2x} + N(t)$". In principle, one might be able to calculate temperature change ΔT based on the data distributed throughout this paper. However, no anthropogenic global warming time series is explicitly presented.

References

87. QSR International, NVivo 12 (v.12.6.0) Qualitative Data Analysis Software (2019), (available at https://qsrinternational.com/nvivo/nvivo-products/).

88. A. Rohatgi, WebPlotDigitizer (v4.4). *https://automeris.io/WebPlotDigitizer* (2020), (available at https://perma.cc/K3AU-DU59).

89. C. P. Morice, J. J. Kennedy, N. A. Rayner, P. D. Jones, Quantifying uncertainties in global and regional temperature change using an ensemble of observational estimates: The HadCRUT4 data set. *J. Geophys. Res. Atmos.* **117**, 1–22 (2012).

90. R. S. Vose, D. Arndt, V. F. Banzon, D. R. Easterling, B. Gleason, B. Huang, E. Kearns, J. H. Lawrimore, M. J. Menne, T. C. Peterson, R. W. Reynolds, T. M. Smith, C. N. Williams, D. B. Wuertz, NOAA's merged land-ocean surface temperature analysis. *Bull.*

Am. Meteorol. Soc. **93**, 1677–1685 (2012).

91. N. J. L. Lenssen, G. A. Schmidt, J. E. Hansen, M. J. Menne, A. Persin, R. Ruedy, D. Zyss, Improvements in the GISTEMP Uncertainty Model. *J. Geophys. Res. Atmos.* **124**, 6307–6326 (2019).
92. R. Rohde, R. A. Muller, R. Jacobsen, E. Muller, S. Perlmutter, A. Rosenfeld, J. Wurtele, D. Groom, C. Wickham, A New Estimate of the Average Earth Surface Land Temperature Spanning 1753 to 2011. *Geoinformatics Geostatistics An Overv.* **01**, 1–7 (2013).
93. K. Cowtan, R. G. Way, Coverage bias in the HadCRUT4 temperature series and its impact on recent temperature trends. *Q. J. R. Meteorol. Soc.* **140**, 1935–1944 (2014).
94. A. Ganopolski, V. Brovkin, Simulation of climate, ice sheets and CO2 evolution during the last four glacial cycles with an Earth system model of intermediate complexity. *Clim. Past*. **13**, 1695–1716 (2017).
95. Trends in Atmospheric Carbon Dioxide (Accessed 6 March 2021). *NOAA Earth Syst. Res. Lab.* (2021), (available at http://gml.noaa.gov/ccgg/trends/data.html).
96. J. Hansen, D. Johnson, A. Lacis, S. Lebedeff, P. Lee, D. Rind, G. Russell, Climate impact of increasing atmospheric carbon dioxide. *Science*. **213**, 957–966 (1981).
97. S. Rahmstorf, G. Foster, N. Cahill, Global temperature evolution: Recent trends and some pitfalls. *Environ. Res. Lett.* **12**, 054001 (2017).
98. S. Lewandowsky, J. S. Risbey, N. Oreskes, The "pause" in global warming: Turning a routine fluctuation into a problem for science. *Bull. Am. Meteorol. Soc.* **97**, 723–733 (2016).
99. J. S. Risbey, S. Lewandowsky, K. Cowtan, N. Oreskes, S. Rahmstorf, A. Jokimäki, G. Foster, A fluctuation in surface temperature in historical context: reassessment and retrospective on the evidence. *Environ. Res. Lett.* **13**, 123008 (2018).
100. B. D. Santer, C. Bonfils, J. F. Painter, M. D. Zelinka, C. Mears, S. Solomon, G. A. Schmidt, J. C. Fyfe, J. N. S. Cole, L. Nazarenko, K. E. Taylor, F. J. Wentz, Volcanic contribution to decadal changes in tropospheric temperature. *Nat. Geosci.* **7**, 185–189 (2014).
101. J. C. Fyfe, V. V. Kharin, B. D. Santer, J. N. S. Cole, N. P. Gillett, Significant impact of forcing uncertainty in a large ensemble of climate model simulations. *PNAS*. **118**, 1–6 (2021).
102. J. M. Gregory, P. M. Forster, Transient climate response estimated from radiative forcing and observed temperature change. *J. Geophys. Res. Atmos.* **113**, 1–15 (2008).
103. B. D. Santer, J. C. Fyfe, S. Solomon, J. F. Painter, C. Bonfils, G. Pallotta, M. D. Zelinka, Quantifying stochastic uncertainty in detection time of human-caused climate signals. *PNAS*. **116**, 19821–19827 (2019).
104. S. Po-Chedley, B. D. Santer, S. Fueglistaler, M. D. Zelinka, P. J. Cameron-Smith, J. F. Painter, Q. Fu, Natural variability contributes to model-satellite differences in tropical tropospheric warming. *PNAS*. **118**, 1–7 (2021).
105. G. Supran, N. Oreskes, Addendum to "Assessing ExxonMobil's climate change communications (1977–2014)." *Environ. Res. Lett.* **15**, 119401 (2020).
106. R. L. Mastracchio, "Controlling Atmospheric CO2" (Internal Document, 1979).

107. W. W. Kellogg, Effects of Human Activities on Global Climate. *Rep. to Exec. Committee, Panel Expert. Clim. Chang. World Meteorol. Organ. Febr. 1977* (1977) (available at https://perma.cc/6G5L-YJ6N).

108. H. Shaw, P. P. McCall, "Exxon Research and Engineering Company's Technological Forecast CO2 Greenhouse Effect" (Internal Document, 1980).

109. M. I. Hoffert, A. J. Callegari, C.-T. Hsieh, The role of deep sea heat storage in the secular response to climatic forcing. *J. Geophys. Res.* **85**, 6667–6679 (1980).

110. ICN, Andrew Callegari biography. *InsideClimate News* (2015), (available at https://perma.cc/8TDU-2MZW).

111. H. S. Kheshgi, A. K. Jain, D. J. Wuebbles, in *Air & Waste Management Association's 90th Annual Meeting & Exhibition, June 8-13 1997, Toronto, Ontario, Canada* (1997).

112. A. K. Jain, H. S. Kheshgi, D. J. Wuebbles, A globally aggregated reconstruction of cycles of carbon and its isotopes. *Tellus*. **48B**, 583–600 (1996).

113. D. L. Albritton, M. R. Allen, P. M. Alfons, J. A. Baede, U. C. Church, D. Xiaosu, D. Yihui, D. H. Ehhalt, C. K. Folland, F. Giorgi, J. M. Gregory, D. J. Griggs, "Climate change 2001: the scientific basis, summary for policymakers. Contribution of Working Group I to the Third Assessment Report of the Intergovernmental Panel on Climate Change" (Cambridge: Cambridge University Press, 2001).

114. H. S. Kheshgi, A. K. Jain, Projecting future climate change: Implications of carbon cycle model intercomparisons. *Global Biogeochem. Cycles*. **17**, 16 (2003).

115. H. Shaw, "CO2 Position Statement" (Internal Document, 1981).

116. H. S. Kheshgi, B. S. White, Does recent global warming suggest an enhanced greenhouse effect? *Clim. Change*. **23**, 121–139 (1993).

117. R. W. Cohen, "Untitled (catastrophic effects letter)" (Internal Document, 1981).

118. R. W. Cohen, D. G. Levine, "Untitled (consensus on CO2 letter) (Internal Document)" (Internal Document, 1982).

119. B. D. Santer, T. M. L. Wigley, T. P. Barnett, E. Anyamba, P. Bloomfield, E. R. Cook, C. Covey, T. J. Crowley, T. Delworth, W. L. Gates, N. E. Graham, J. M. Gregory, "Detection of Climate Change and Attribution of Causes. Contribution of Working Group I of the Second Assessment Report of the Intergovernmental Panel on Climate Change, Chapter 8" (Cambridge: Cambridge University Press, 1996).

Table S1. Sensitivity analyses of accuracy and modeling skill of ExxonMobil's global warming projections in comparison to subsequent observed temperature changes, subject to: (column 4) exclusion of the two (out of 16) projections reported by ExxonMobil scientists that overlap with the 18 academic and government climate model projections analyzed by Hausfather *et al.* (2020); and (column 5) inclusion only of the 12 (out of 16) temperature projections specifically output by models built or run in-house by ExxonMobil scientists, indicated by asterisks in Figs. 1–3 and Table 1. As described in section S1.2.5, for each of the above subsets of data, sensitivity analyses are performed by recalculating all reported statistics: (1) average predicted global warming; (2) uncertainty of global warming projections (bootstrapped two-sigma standard error of the mean); (3) fraction of projections consistent with historical observations (out of all projections corresponding to: (top line) each forcing scenario as independent; (bottom line) each unique graph and table as independent); and (4) average skill score. (3) and (4) are computed for both temperature-versus-time and implied transient climate response (iTCR) metrics.

Metric	Statistic	All projections	All projections, less two overlaps with Hausfather *et al.* (2020)	Projections modeled by ExxonMobil scientists
Temperature change versus time	Average warming (°C per decade)	0.20 ± 0.04	0.20 ± 0.04	0.18 ± 0.04
	Standard error of warming projections (%)	±21	±22	±21
	Projections consistent with observations	10/16 (62.5%) 10/12 (83.3%)	8/14 (57.1%) 8/10 (80%)	6/12 (50%) 6/8 (75%)
	Average skill score (%)	67 ± 7	65 ± 8	72 ± 6
Implied transient climate response (iTCR)	Projections consistent with observations	12/16 (75%) 9/12 (75%)	10/14 (71.4%) 7/10 (70%)	9/12 (75%) 6/8 (75%)
	Average skill score (%)	67 ± 9	64 ± 9	75 ± 5

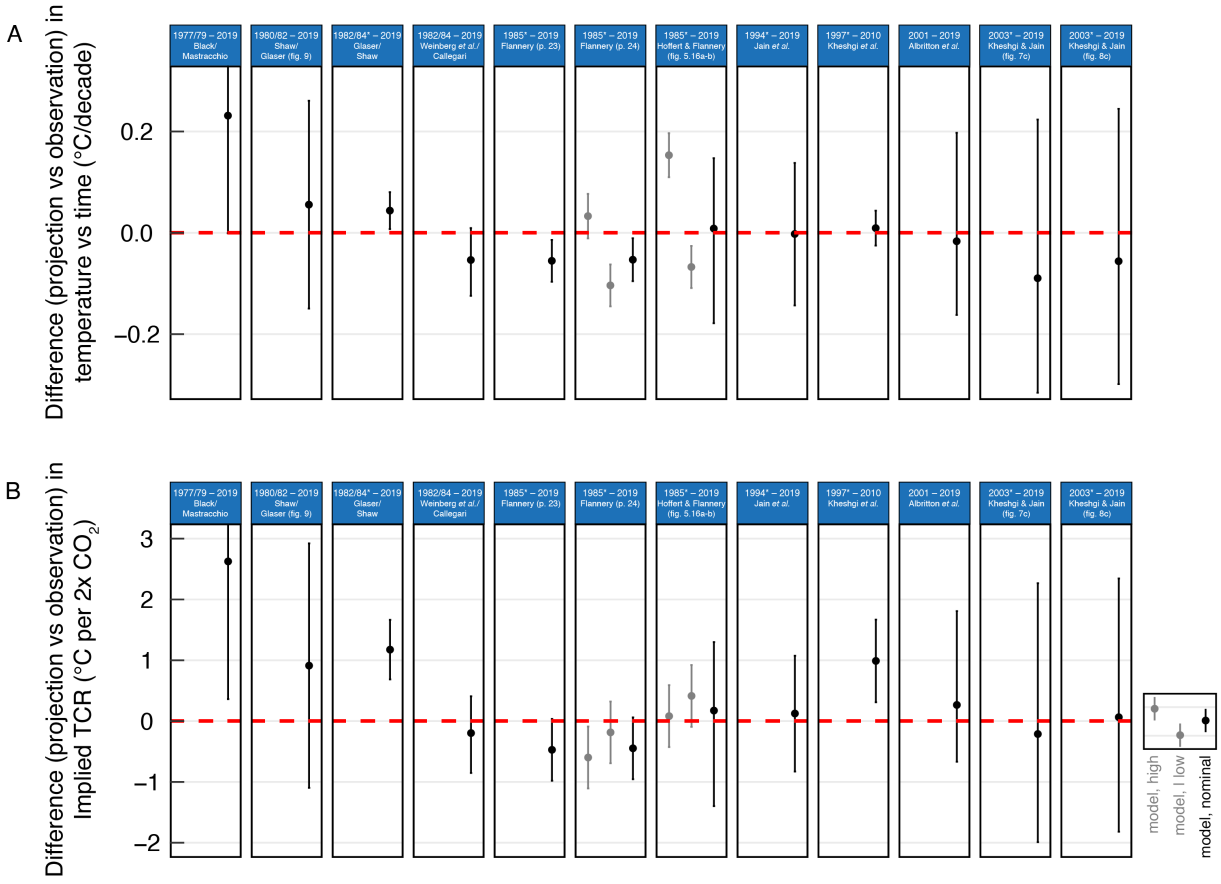

Fig. S1. Differences between (i) historical observations and (ii) projections reported by ExxonMobil scientists in internal documents and peer-reviewed publications in terms of (A) temperature change versus time and (B) temperature change versus change in radiative forcing ("implied TCR"). Differences are computed over model projection periods indicated in the blue boxes above each panel. Asterisks indicate global warming projections modeled by ExxonMobil scientists themselves.

Table S2. Catalog of analyzed internal documents.

Date	Authors	Title
31 October 1977	Shaw, H. to Harrison, J. W.	Environmental Effects of Carbon Dioxide
06 June 1978	Black, J. to Turpin, F. G. (cc: Alpert, N. et al.)	The Greenhouse Effect
07 December 1978	Shaw, H. to David Jr., E. E.	Untitled (request for a credible scientific team)
07 March 1978	Weinberg, H. N. to Gornowski, E. J.	CO2
26 March 1979	Garvey, E. A., Shaw, H., Broecker, W. S., Takahashi, T. presentation to Machta, L.	Proposed Exxon Research Program to Help Assess the Greenhouse Effect
16 October 1979	Mastracchio, R. L. to Hirsch, R. L. (cc: Black, J. F. et al.)	Controlling Atmospheric CO2
19 November 1979	Shaw, H. to Weinberg, H. N. (cc: Werthamer, N. R.)	Research in Atmospheric Science
29 January 1980	Eckelmann, W. R. to O'Loughlin, M. E. J. (cc: David, E. E. et al.)	Exxon's View and Position on "Greenhouse Effect"
09 June 1980	Weinberg, H. N. to Shaw, H. and Werthamer, N. R.	Greenhouse Program
08 July 1980	Werthamer, N. R. to Weinberg, H. N.	CO2 Greenhouse Communications Plan
18 December 1980	Shaw, H. to Kett, R. K. (cc: McCall, P. P. et al.)	Exxon Research and Engineering Company's Technological Forecast CO2 Greenhouse Effect
03 February 1981	Gervasi, G. R. to Northington, G. A. (cc: Preston, R. L. et al.)	CO2 Emissions Natuna Gas Project
05 February 1981	Long, G. H. to Lucceshi, P. J. et al. (cc: Barnum, R. E. et al.)	Atmospheric CO2 Scoping Study
15 May 1981	Shaw, H. to David Jr., E. E. (cc: Barnum, R. E. et al.)	CO2 Position Statement
18 August 1981	Cohen, R. W. to Glass, W. (cc: Weinberg, H. N. et al.)	Untitled (catastrophic effects letter)
18 June 1982	Natkin, A. M. to Weinberg, H. N. (cc: Forshee, M. E. et al.)	CRL/CO2 Greenhouse Program
14 July 1982	Cohen, R. W. to Kimon, P. (cc: Berner, R. et al.)	Untitled (Esso project terminated letter)
21 July 1982	Weinberg, H. N., Cohen, R. W., Callegari, A. J., Flannery, B., et al.	CO2-Greenhouse Effect; Corporate Research Climate Modeling
02 September 1982	Cohen, R. W., Levine, D. G. to Natkin, A. M. (cc: Callegari, A. J. et al.)	Untitled (consensus on CO2 letter)
12 November 1982	Glaser, M. B. to Cohen, R. W. et al.	CO2 "Greenhouse" Effect
17 October 1983	Natkin, A. M. to Preston, R. L. (Esso Eastern) (cc: Gervasi, G. R. et al.)	Untitled (ocean storage environmental concerns letter)
27 October 1983	Gervasi, G. R. to Downing, R. G. et al. (cc: Gates, D. F. et al.)	Background Paper Environmental Issues Natuna Gas Project
1984	Flannery, B., Callegari, A. J., Nair, B., Roberge, W. G.	The Fate of CO2 from the Natuna Gas Project if Disposed of by Subsea Sparging
02 February 1984	Callegari, A. J.	Corporate Research Program in Climate/CO2-Greenhouse
28 March 1984	Shaw, H.	CO2 Greenhouse and Climate Issues (EUSA/ER&E Environmental Conference, Florham Park, New Jersey)
07 May 1985	Shaw, H., Henrikson, F. W. to Lab Directors/Program Managers (cc: Cohen, R. W. et al.)	CR Interactions (handout for June 12th meeting with Lee Raymond)
04 October 1985	Flannery, B. P.	CO2 Greenhouse Update 1985
08 March 1988	Carlson, J. M. to Levine, D. G.	The Greenhouse Effect
02 February 1989	Levine, D. G.	Potential Enhanced Greenhouse Effects, Status and Outlook (Presentation to the Board of Directors of Exxon Corp)
Fall 1989	Flannery, B. P.	Greenhouse Science (CONNECTIONS ExxonMobil publication - "Proprietary information for company use only")
21 December 1995	Bernstein, L. S. to Members of Global Climate Coalition	Primer on Climate Change Science
18 March 2002	Flannery, B. P. to Cooney, P. and Marburger, J. (cc: Randol, A. G.)	Activities

Table S3. Catalog of analyzed peer-reviewed publications.

Year	Authors	Title	Publication
1982	Garvey, E. A., Prahl, F., Nazimek, K., Shaw, H.	Exxon global CO2 measurement system	IEEE Transactions on Instrumentation and Measurement
1983	Hoffert, M.I., Flannery, B. P., Callegari, A. J., Hseih, C. T., Wiscombe, W.	Evaporation-limited tropical temperatures as a constraint on climate sensitivity	Journals of the Atmospheric Sciences
1984	Flannery, B. P.	Energy balance models incorporating transport of thermal and latent energy	Journals of the Atmospheric Sciences
1984	Flannery, B. P., Callegari, A. J., Hoffert M. I.	Energy balance models incorporating evaporative buffering of equatorial thermal response	Geophysical Monograph Series: Climate Processes and Climate Sensitivity
1985	Flannery, B. P., Callegari, A. J., Hoffert, M. I., Hseih, C. T., Wainger, M. D.	CO2 driven equator-to-pole paleotemperatures: predictions of an energy balance model with and without a tropical evaporation buffer	The Carbon Cycle and Atmospheric CO2: Natural Variations Archean to Present, Geophysical Monograph 32
1985	Hoffert, M. I., Flannery, B. P. (eds. MacCracken, M. C., Luther, F. M.)	Model Projections of the Time-Dependent Response to Increasing Carbon Dioxide	Projecting the Climatic Effects of Increasing Carbon Dioxide, United States Department of Energy
1988	Thomas, E. R., Denton, R. D.	Conceptual studies for CO2/natural gas separation using the controlled freeze zone (CFZ) process	Gas Separation and Purification
1991	Kheshgi, H. S., Hoffert, M. I., Flannery, B. P.	Marine biota effects on the compositional structure of the world oceans	J. Geophys. Res.
1993	Kheshgi, H. S., White, B. S.	Effect of climate variability on estimation of greenhouse parameters: usefulness of a pre-instrumental temperature record	Quaternary Science Reviews
1993	Flannery, B. P., Kheshgi, H. S., Hoffert, M. I., Lapenis, A. G.	Assessing the effectiveness of marine CO2 disposal	Energy Convers. Mgmt
1993	Kheshgi, H. S., White, B. S.	Does recent global warming suggest an enhanced greenhouse effect?	Climatic Change
1994	Jain, A. K., Kheshgi, H. S., Wuebbles, D. J.	Integrated Science Model for Assessment of Climate Change	94-TP59. 08, Air and Waste Management Assoc.; also Lawrence Livermore Nat. Lab., UCRL-JC-116526, Natl. Technical Info Service, US Dept. of Commerce. Proceedings of the 87th Annual Meeting of the Air & Waste Management Association
1994	Kheshgi, H. S., Flannery, B. P., Hoffert, M. I., Lapenis, A. G.	The effectiveness of marine CO2 disposal	Energy
1995	Jain, A. K., Kheshgi, H. S., Hoffert, M. I., Wuebbles, D. J.	Distribution of radiocarbon as a test of global carbon cycle models	Global Biogeochem. Cycles
1995	Kheshgi, H. S.	Sequestering atmospheric carbon dioxide by increasing ocean alkalinity	Energy
1996	Santer, B. D., Wigley, T.M.L., Barnett, T.P., Anyamba, E.,…, Kheshgi, H.S. (Contributor), et al.	Detection of Climate Change and Attribution of its Causes	Intergovernmental Panel on Climate Change Second Assessment Report, Chapter 8, Volume I
1996	Kheshgi, H. S., White, B.S.	Modelling ocean carbon cycle with a nonlinear convolution model	Tellus
1996	Kheshgi, H. S., Lapenis, A. G.	Estimating the accuracy of Russian paleotemperature reconstructions	Palaeogeography, Palaeoclimatology, Palaeoecology
1996	Kheshgi, H. S., Jain, A. K., Wuebbles, D. J	Accounting for the missing carbon sink with the CO2 Fertilization Effect	Climatic Change
1996	Jain, A. K., Kheshgi, H. S., Wuebbles, D. J	A globally aggregated reconstruction of cycles of carbon and its isotopes	Tellus
1996	Prince, R. C., Kheshgi, H. S.	Longevity in the deep	Trends in Ecology & Evolution
1997	Jain, A. K., Kheshgi, H. S., Wuebbles, D. J.	Is there an imbalance in the global budget of bomb-produced radiocarbon?	Journal of Geophysical Research
1997	Archer, D., Kheshgi, H., Maier-Reimer, E.	Multiple Timescales for the Neutralization of Fossil Fuel CO2	Geophysical Research Letters
1997	Kheshgi, H. S., Schlesinger, M. E., Lapenis, A. G.	Comparison of Paleotemperature Reconstructions as Evidence for the Paleo-Analog Hypothesis	Climatic Change
1997	Kheshgi, H.S., Jain, A. K., Wuebbles, D. J.	Analysis of proposed CO2 emission reductions in the context of stabilization	Proceedings of the Air & Waste Management Association's 90th Annual

		of CO2 concentration	Meeting & Exhibition.
1998	Archer, D., Kheshgi, H., Maier-Reimer, E.	The dynamics of fossil fuel CO2 neutralization by marine CaCO3	Global Biogeochemical Cycles
1998	Hayhoe, K. A. S., Kheshgi, H. S., Jain, A. K., Wuebbles, D. J.	Trade-Offs in Fossil Fuel Use: The Effects of CO2 , CH4 and SO2 Aerosol Emissions on Climate	World Resource Review
1999	Kheshgi, H. S., Jain, A. K., Kotamarthi, V. R. Wuebbles, D. J.	Future Atmospheric Methane Concentrations in the Context of the Stabilization of Greenhouse Gas Concentrations	J. Geophys. Res.
1999	Kheshgi, H. S., Jain, A. K., Wuebbles, D. J.	Model-based estimation of the global carbon budget and its uncertainty from carbon dioxide and carbon isotope records	J. Geophys. Res.,
2000	Kheshgi, H. S., Prince, R. C., Marland, G.	The Potential of Biomass Fuels in the Context of Global Change: Focus on Transportation Fuels	Annual Review of Energy and the Environment
2000	Watson, R.,…, Kheshgi, H. et al. (eds. Watson, R. T. et al.)	Land Use, Land-Use Change, and Forestry	A Special Report of the Intergovernmental Panel on Climate Change
2000	Hayhoe, K. A. S., Jain, A. K., Kheshgi, H. S., Wuebbles, D. J.	Contribution of CH4 to Multi-Gas Reduction Targets: The Impact of Atmospheric Chemistry on GWPs	Non-CO2 Greenhouse Gases: Scientific Understanding, Control and Implementation, 425-432. Proceedings of the Second International Symposium, Noordwijkerhout, The Netherlands, 8–10 September 1999
2001	Bolin, B., Kheshgi, H. S.	On strategies for reducing greenhouse gas emissions	PNAS
2001	Kheshgi, H. S., B. S. White	Testing Distributed Parameter Hypotheses for the Detection of Climate Change	Journal of Climate
2001	Prentice, C., Farquhar, G., Fasham, M., Goulden, M., Heimann, M., Jaramillo, V., Kheshgi, H., Quéré, C. L., Scholes, R., Wallace, D.	The carbon cycle and atmospheric CO2	Intergovernmental Panel on Climate Change Third Assessment Report, Working Group 1, Chapter 3
2001	Mitchell, J. F. B.,...,Kheshgi, H. S. (Contributing Author), et al.	Detection of Climate Change and Attribution of its Causes	IPCC TAR WGI Ch12
2001	Albritton, D. L.,...,Kheshgi, H.S. (Contributing Author), et al.	Technical Summary	Intergovernmental Panel on Climate Change Third Assessment Report, Working Group 1, Summary for Policymakers and Technical Summary
2001	Kauppi, P.,...,Kheshgi, H. S. (Contributing Author), et al.	Technical and Economic Potential of Options to Enhance, Maintain and Manage Biological Carbon Reservoirs and Geo-Engineering	Intergovernmental Panel on Climate Change Third Assessment Report, Working Group 3, Chapter 4
2001	Toth, F. L,..., Flannery, B. (Lead Author), et al.	Decision Making Frameworks	Intergovernmental Panel on Climate Change Third Assessment Report, Working Group 3, Chapter 10
2002	Hayhoe, K. A. S., Kheshgi, H. S., Jain, A. K., Wuebbles, D. J.	Substitution of natural gas for coal: climatic effects of utility sector emissions	Climatic Change
2002	Hoffert, M. I., Caldeira, K., Benford, G., Criswell, D. R., Green, C., Herzog, H., Jain, A. K., Lackner, K. S., Lewis, J. S., Lightfoot, H. D., Manheimer, W., Mankins, J. C., Mauel, M. E., Perkins, L. J., Schlesinger, M. E., Volk, T., Wigley, T. M. L.	Advanced technology paths to global climate stability: energy for a greenhouse planet	Science
2003	Kheshgi, H. S., Jain, A. K.	Projecting future climate change: implications of carbon cycle model intercomparisons	Global Biogeochemical Cycles
2003	Le Quéré, C., Aumont, O., Bopp, L., Bousquet, P., Ciais, P., Francey, R., Heimann, M., Keeling, C. D., Keeling, R. F., Kheshgi, H., Peylin, P., Piper, S. C., Prentice, I. C., Rayner, P. J.	Two decades of ocean CO2 sink and variability	Tellus
2004	Kheshgi, H. S., Archer, D.	A non-linear convolution model for the	Journal of Geophysical Research

		evasion of CO2 injected into the deep ocean	
2004	Kheshgi, H. S.	Evasion of CO2 injected into the ocean in the context of CO2 stabilization	Energy
2004	Kheshgi, H. S.	Ocean carbon sink duration under stabilization of atmospheric CO2: a 1,000-year time-scale	Geophysical Research Letters
2005	Kheshgi, H. S., Prince, R.	Sequestration of fermentation CO2 from ethanol production	Energy
2005	Kheshgi, H.S., Smith, S.J., Edmonds, J.A.	Emissions and Atmospheric CO2 Stabilization: Long-term Limits and Paths	Mitigation and Adaptation Strategies
2005	Prince, R.C., Kheshgi, H.S.	The photobiological production of hydrogen: potential efficiency and effectiveness as a renewable fuel	Critical Reviews in Microbiology
2005	Caldeira, K., Akai, M., Brewer, P., Chen, B., Haugan, P., Iwama, T., Johnston, P., Kheshgi, H., Li, Q., Ohsumi, T., Poertner, H., Sabine, C., Shirayama, Y., Thomson, J.	Ocean storage (Chapter 6)	IPCC Special Report on Carbon Dioxide Capture and Storage
2007	Barker, T., Bashmakov, I., Alharthi, A., Amann, M., Cifuentes, L., Drexhage, J., Duan, M., Edenhofer, O., Flannery, B., Grubb, M., Hoogwijk, M., Ibitoye, F. I., Jepma, C. J., Pizer, W. A.	Mitigation from a cross-sectoral perspective	Intergovernmental Panel on Climate Change Fourth Assessment Report, Working Group 3, Chapter 11
2007	Kheshgi, H. S. (eds. Schlesinger, M. E., Kheshgi, H., Smith, J. B., de la Chesnaye, F. C., Reilly, J. M., Wilson, T. and Kolstad, C.)	Probabilistic estimates of climate change: methods, assumptions and examples (p. 49-61)	Human-Induced Climate Change: An Interdisciplinary Assessment
2007	Kheshgi, H. S. (Coordinating Editor for Part 1) (eds. Schlesinger, M. E., Kheshgi, H., Smith, J. B., de la Chesnaye, F. C., Reilly, J. M., Wilson, T. and Kolstad, C.)	Part 1, Climate System Science (p. 2-3)	Human-Induced Climate Change: An Interdisciplinary Assessment
2007	Ribeiro, S. K.,..., Kheshgi, H. (Review Editor), et al.	Transport and its infrastructure	Intergovernmental Panel on Climate Change Fourth Assessment Report, Working Group 3, Chapter 5
2009	Lively, R. P., Chance, R. R., Kelley, Deckman, H. W., Drese, J. H., Jones, C. W., Koros, W. J.	Hollow fiber adsorbents for CO2 removal from flue gas	Ind. Eng. Chem. Res.
2009	Jain, A., Yang, X., Kheshgi, H., McGuire, A. D., Post, W., Kicklighter, D.	Nitrogen attenuation of terrestrial carbon cycle response to global environmental factors	Global Biogeochemical Cycles
2009	Benge, G.	Improving wellbore seal integrity in CO2 injection wells	Energy Procedia
2009	Hershkowitz, F., Deckman, H. W., Frederick, J. W., Fulton, J. W., Socha, R. F.	Pressure swing reforming: a novel process to improve cost and efficiency of CO2 capture in power generation	Energy Procedia
2009	Kheshgi, H. S., Crookshank, S., Cunha, P., Lee, A., Bernstein, L., Siveter, R.	Carbon capture and storage business models	Energy Procedia
2009	Northrop, P. S., Valencia, J. A.	The CFZTM process: a cryogenic method for handling high-CO2 and H2 S gas reserves and facilitating geosequestration of CO2 and acid gases	Energy Procedia
2009	Parker, M. E., Meyer, J. P., Meadows, S.	Carbon dioxide enhanced oil recovery injection operations technologies	Energy Procedia
2009	Ritter, K., Siveter, R., Lev-On, M., Shires, T., Kheshgi, H.	Harmonizing the quantification of greenhouse gas emission reductions through oil and gas industry project guidelines	Energy Procedia
2009	Wilkinson, J., Szafranski, R., Lee, K. -S., Kratzing, C.	Subsurface design considerations for carbon dioxide storage	Energy Procedia
2009	Xiao, Y., Xu, T., Pruess, K.	The effects of gas-fluid-rock interactions on CO2 injection and storage: insights from reactive transport modeling	Energy Procedia
2011	Flannery, B.P.	Comment (on the scale-up of carbon dioxide capture and storage technology systems)	Energy Economics

2011	Burgers, W. F. J., Northrop, P. S., Kheshgi, H. S., Valencia, J. A.	Worldwide development potential for sour gas	Energy Procedia
2011	Parker, M. E., Northrop, S., Vaencia, J. A., Foglesong, R. E., Duncan, W. T.	CO2 management at ExxonMobil's LaBarge field, Wyoming, USA	Energy Procedia
2012	Kheshgi, H., Thomann, H., Bhore, N. B., Hirsh, R. B., Parker, M. E., Teletzke, G. F.	Perspectives on CCS cost and economics	SPE Economics & Management
2014	Allen, R. J., Landuyt, W.	The vertical distribution of black carbon in CMIP5 models: Comparison to observations and the importance of convective transport	J. Geophys. Res. Atmos.
2014	Song, Y., Jain, A. K., Landuyt, W., Kheshgi, H. S., Khanna, M.	Estimates of Biomass Yield for Perennial Bioenergy Grasses in the United States Industry	BioEnergy Research
2014	Fischedick M., Roy, J., Abdel-Aziz, A., Acquaye, A., Allwood, J. M., Ceron, J. - P., Geng, Y., Kheshgi, H., Lanza, A., Perczyk, D., Price, L., Santalla, E., Sheinbaum, C., Tanaka, K. (eds. O. Edenhofer, R. Pichs-Madruga, Y. Sokona, E. Farahani, S. Kadner, K. Seyboth, A. Adler, I. Baum, S. Brunner, P. Eickemeier, B. Kriemann, J. Savolainen, S. Schlömer, C. von Stechow, T. Zwickel and J.C. Minx)		Intergovernmental Panel on Climate Change Fifth Assessment Report, Working Group 3, Chapter 11
2014	Arent, D. J.,..., Kheshgi, H. (Review Editor), et al.	Key economic sectors and services	Intergovernmental Panel on Climate Change Fifth Assessment Report, Working Group 2, Chapter 10

Document category	Publication year	First author, title	Quotation and notes	Predicted year
Internal	1979	Mastracchio, 'Controlling Atmospheric CO_2' (*33*)	"No limit on CO_2 emissions" scenario: "Noticeable temperature changes would occur around 2010 as the concentration reaches 400 ppm." "CO_2 Increase Limited to 510 ppm" scenario: "Noticeable temperature changes would occur around 2010 when the CO_2 concentration reaches 400 ppm."	2010
Internal	1980	Shaw, 'Exxon Research and Engineering Company's Technological Forecast CO_2 Greenhouse Effect' (*36*)	"Projections on When General Consensus Can be Reached. It is anticipated by most scientists that a general consensus will not be reached until such time as a significant temperature increase can be detected above the natural random temperature fluctuations in average global climate. The earliest that such discreet signals will be able to be measured is after the year 2000."	2000
Internal	1981	Cohen, Untitled (catastrophic effects letter) (*53*)	"The models that appear most credible (to us) do predict measurable changes in temperature, rainfall pattern, and sea-level by the year 2030 for the postulated fossil fuel combustion rates…"	2030
Internal	1981	Shaw, 'CO_2 Position Statement' (*50*)	"An indication of the average global temperature increase due to CO2 will not be measurable above normal climatic fluctuations (noise) until about 2000."	2000
Internal	1982	Cohen, Untitled (consensus on CO_2 letter) (*54*)	"It is generally believed that the first unambiguous CO_2-induced temperature increase will not be observable until around the year 2000."	2000
Internal	1982	Glaser, 'CO_2 "Greenhouse" Effect' (*37*)	"If the earth is on a warming trend, we're not likely to detect it before 1995. This is about the earliest projection of when the temperature might rise the 0.5 needed to get beyond the range of normal temperature fluctuations. On the other hand, if climate modeling uncertainties have exaggerated the temperature rise, it is possible that carbon dioxide induced "greenhouse effect" may not be detected until 2020 at the earliest." "Detection of a CO_2 Greenhouse Effect...A number of climatologists claim that they are currently measuring a temperature signal (above climate noise) due to a CO_2 induced greenhouse effect, while the majority do not expect such a signal to be detectable before the year 2000... Based on these estimates, one concludes that a doubling of current concentrations of CO_2 will probably not cause an average global temperature rise much in excess or 3 C, or the effect should be detectable at the present time [1979]. Alternatively, if the greenhouse effect is not detected until 2000, then the temperature due to a CO_2 doubling will probably be under 2 C. Using the Exxon 21st Century Study as a basis for fossil fuel growth patterns, the average global temperature increases due to CO_2 would range between 0.8 and 1.6 C by 2030. A doubling of atmospheric CO_2 would be extrapolated from the fossil fuel consumption rates of the 21st Century Study to occur at about the year 2090 with the temperature increase ranging between 1.3° and 3.1°C." This suggests that the most likely window for detecting warming is 1995-2000. We take the central estimate of 1997.5.	1997.5
Internal	1982	Weinberg *et al.*, 'CO_2-Greenhouse Effect; Corporate Research Climate Modeling' (*39*)	"FIRST EFFECTS PREDICTED BY YEAR 2000", alongside corresponding figure from Hansen *et al.* 1981 (not explicitly cited).	2000
Internal	1984	Callegari, 'Corporate Research Program in Climate/CO_2-Greenhouse' (*40*)	"FIRST EFFECTS PREDICTED BY YEAR 2000", alongside corresponding cited figure from Hansen *et al.* 1981.	2000
Internal	1984	Shaw, 'CO_2 Greenhouse and Climate Issues' (EUSA/ER&E Environmental Conference, Florham Park, New Jersey) (*38*)	"WE MUST ESTIMATE WHEN THE CO_2 EFFECT WILL EXCEED THE CLIMATIC NOISE THRESHOLD OF 0.5C...MOST CLIMATOLOGISTS ASSUME THAT THE CO_2 EFFECT WILL BE DETECTABLE BY THE YEAR 2000."	2000

Internal	1985	Flannery, 'CO_2 Greenhouse Update 1985' (*41*)	"EMERGING DILEMMA FOR CLIMATE MODELS: WHY HASN'T WARMING BEEN OBSERVED?" States that for a climate sensitivity corresponding to 2-3C temperature rise, warming between 1850-1980 should be "0.8 C marginally detectable"; and that for a climate sensitivity corresponding to 4-5C temperature rise, warming between 1850-1980 should be "1.6 C readily detectable". "Proposed solution, delay from oceanic thermal buffering much greater than found in previous studies." "CONCLUSIONS FROM 1 D OCEAN MODEL...Response delayed by decades, 30 years, not centuries". Since it is suggested that warming should have been somewhere between "marginally" and "readily" detectable by 1980 (probably closer to "readily" because "Recent GCM models predict greater sensitivity"), the implied date for detectable warming is ~1980+30 = 2010.	2010
Peer-reviewed	1985	Hoffert & Flannery, 'Projecting the Climatic Effects of Increasing Carbon Dioxide', United States Department of Energy (*44*)	"The conventional wisdom is that the systematically increasing CO_2 temperature signal will emerge from the background noise in the next 10-15 years (NRC 1983). This would be a plausible conclusion from existing models if the noise were truly random, but it may not be the case...If all of the forcing factors could be modeled explicitly, it might be possible to extract the CO_2 signal from historical data sets as the residual variation, that is, removing those variations that we may be able to explain (e.g., volcanic effects) may make more apparent the CO_2 signal that would normally remain hidden in formal statistical analyses. Such superpositions of effects, for example, are the basis of transient model calculations of Hansen *et al.* (1981), which show apparent agreement with a particular historical data set and which have been cited widely in popular accounts as being consistent with the fossil fuel CO_2 greenhouse theory (Sullivan 1981; Revelle 1982, etc.)." This suggests detectable warming within 10-15 years of 1985, i.e. 1985-2000. We take the central estimate of 1992.5.	1992.5
Peer-reviewed	1996	Santer *et al.*, Intergovernmental Panel on Climate Change Second Assessment Report, Chapter 8, Volume I (*55*)	"The body of statistical evidence in Chapter 8…now points towards a discernible human influence on global climate."	N/A
Peer-reviewed	2001	Albritton *et al.*, Intergovernmental Panel on Climate Change Third Assessment Report, Working Group 1, Summary for Policymakers and Technical Summary (*48*)	"There is new and stronger evidence that most of the warming observed over the last 50 years is attributable to human activities."	N/A
Median predicted year when anthropogenic global warming first detectable				2000 ± 5

Table S4. Predicted years when anthropogenic global warming would first be detectable, as reported in ExxonMobil internal and peer-reviewed publications. The predicted years are inferred from the corresponding supporting document quotations. The second and third IPCC reports, to which the company's chief climate scientist was a contributing author, are tabulated for completeness but are not included in the calculation of the average predicted year because those reports determined that human-caused global warming was already discernible.

(S4) Online Repository

Raw numerical data resulting from digitization of all analyzed original PDF datasets are deposited on Harvard Dataverse at https://doi.org/10.7910/DVN/R4MOAE (*56*). The code used to generate the results of this study are provided in the same repository.